

On the application of fiber optic gyroscopes for detection of seismic rotations

Alexander Velikoseltsev · Karl Ulrich Schreiber · Alexander Yankovsky ·
Jon-Paul R. Wells · Alexander Boronachin · Anna Tkachenko

Received: 18 July 2011 / Accepted: 26 January 2012 / Published online: 18 February 2012
© Springer Science+Business Media B.V. 2012

Abstract In recent years, the measurement of rotational components of earthquake-induced ground motion became a reality due to high-resolution ring laser gyroscopes. As a consequence of the fact that they exploit the Sagnac effect, these devices are entirely insensitive to translational motion and are able to measure the

rotation rate with high linearity and accuracy over a wide frequency band. During the last decade, a substantial number of earthquakes were recorded by the large ring lasers located in Germany, New Zealand, and USA, and the subsequent data analysis demonstrated reliability and consistency of the results with respect to theoretical models. However, most of the observations recorded teleseismic events in the far-field. The substantial mass and the size of these active interferometers make their near-field application difficult. Therefore, the passive counterparts of ring lasers, the fiber optic gyros can be used for seismic applications where the mobility is more important than extreme precision. These sensors provide reasonable accuracy and are small in size, which makes them perfect candidates for strong motion applications. The other advantage of fiber optic gyroscopes is that if the earthquake is local and shallow (like one occurred early this year at Canterbury, New Zealand), the large ring lasers simply do not have the dynamic range—the effect is far too large for these instruments. In this paper, we analyze a typical commercially available tactical grade fiber optic gyroscope (VG-951) with respect to the seismic rotation measurement requirements. The initial test results including translation and upper bounds of seismic rotation sensitivity are presented. The advantages and limitations of tactical grade fiber optic gyroscope as seismic rotation sensor are discussed.

A. Velikoseltsev (✉) · A. Boronachin · A. Tkachenko
Department of Laser Measurement and Navigation
Systems, Saint Petersburg Electrotechnical University,
Prof. Popov str. 5, St.-Petersburg, 197376, Russia
e-mail: avelikoseltsev@gmail.com

A. Boronachin
e-mail: AMBoronachin@mail.eltech.ru

A. Tkachenko
e-mail: tkachenko_nv@mail.ru

K. U. Schreiber
Bundesamt für Kartographie und Geodäsie,
Geodätisches Observatorium Wettzell, 93444
Bad Kötzing, Germany
e-mail: schreiber@fs.wettzell.de

A. Yankovsky
D.I. Mendeleev Institute for Metrology,
Moskovsky pr., 19, St.-Petersburg, 190005, Russia
e-mail: A.Yankovsky@vniim.ru

J.-P. R. Wells
Department of Physics and Astronomy, University of
Canterbury, Private Bag 4800, Christchurch 8020,
New Zealand
e-mail: jon-paul.wells@canterbury.ac.nz

Keywords Rotational ground motion · Fiber optic gyroscope · Rotational seismology

1 Introduction

Six independent degrees of freedom, i.e., three degrees of linear motion and three degrees of rotational motions are enough to describe the movement of a rigid body in space and are widely used for the navigation of airborne and surface vehicles, where a triad of accelerometers delivers measurements of linear motion and a triad of gyroscopes measures the angular motion, respectively. Reliable recordings of rotational signals induced by remote earthquakes became first available with development of large ring lasers (Pancha et al. 2000). Further improvement in the design of large ring lasers allowed the detection of rotational signals with great detail even from distant earthquakes with sufficient magnitude. The consistency of jointly observed rotational and translational seismic motion has been explicitly shown (Igel et al. 2005). The analysis of co-located earthquake recordings obtained from a large ring laser and an array of seismometers demonstrated the complications of traditional methods for deriving rotations and suggested the development of field-deployable rotation sensor (Suryanto et al. 2006).

The fiber optic gyroscope (FOG) is not sensitive enough to measure rotational signals from distant earthquakes, but may be used as a device for strong motion field measurements and for the measurement of building behavior under the influence of an earthquake. The advantage of FOGs over other types of rotational sensors, which utilize an inertial mass as the reference, is the same as that of the ring laser; it is insensitive to translational motion. Other types of instruments, which are capable of detecting rotation or rotation variations, suffer from susceptibility to translations, cross-axis sensitivity, and non-linearity of the output signal. FOG-based sensor assemblies may also be susceptible to latter two effects; however, these can be estimated by means of special test procedures, well established in navigation sensors manufacturing processes. Recent studies on a shake table have demonstrated the suitability of these devices (Schreiber et al. 2009).

In the case of the strong seismic signals (near-field event), the rotation measurement system based on a FOG can fulfil two purposes. Firstly, it naturally provides the detection of rotations around all three axes and thereby fills the currently existing gap in available seismic information. It should be noted that among the optical rotation sensors, the FOG is the most viable candidate in the case of very strong local seismic event, as large ring lasers (mostly those built as heterolithic structures) would go out of alignment immediately after the first shock. The small-sized monolithic ring lasers could also be used for such application; however, these are rather expensive and not entirely reliable due to the requirement of mechanical dither for lock-in compensation (Aronowitz 1999). A number of other technologies exist for detection of strong seismically induced rotations (Takamori et al. 2009; Cowsik et al. 2009; Nigbor et al. 2009). In this paper, we focus on optical devices, which possess some unique features that make them perfect for pure rotation sensing. Secondly, it also provides tilt corrections for seismometers, since a FOG is sensitive to rotations only. The tilt may reach tenths of degrees in strong motion applications and could produce significant baseline shifts, which show up as a large displacement (Graizer 2006a, 2010). Shifts of several meters, especially for the horizontal components, may be the result (Boore 2001; Pillet and Virieux 2007). It is difficult to distinguish between horizontal accelerations and tilt in case of near field measurements. Therefore, the independent recording of angular motion by suitable sensors, sensitive to rotations *only*, can be very helpful for the understanding of strong near field seismic events (Graizer 2006b).

2 Fiber optic gyroscope operation principle

The operation of the passive interferometric fiber optic gyroscope is based on the Sagnac effect, which reveals itself as a phase shift between two counter-propagating light beams inside the closed fiber coil in the presence of externally applied rotational motion around its sensitive plane (Lefevre 1993). The observed phase shift is di-

rectly proportional to the rotation rate Ω and can be expressed as

$$\Delta\varphi = \frac{2\pi LD}{\lambda c} \cdot \Omega \quad (1)$$

where λ is the wavelength of the light, c is the velocity of light, D is mean fiber coil diameter, and $L = \pi ND$ is the total length of the fiber with N turns. As it can be seen from the Eq. 1, one can improve the resolution of the device by increasing the number of turns N . This design flexibility allows for a variety of instrumental operation settings, while preserving its wide dynamic range.

The sensitivity limit of the fiber optic gyro is defined by the photon shot noise and the relative intensity noise (Lawrence 1998). The first limit is a fundamental threshold, while the second mechanism is usually dominating at higher powers and broader spectral linewidth of the applied light source. Currently, FOGs can deliver performance values as high as 5.5×10^{-8} rad/s (Sanders and Szafraniec 1999). However, most of the tactical and navigation grade units work in the range of 10^{-6} – 10^{-7} rad/s.

3 Prerequisites for seismic rotation measurements

The magnitude of rotational ground motion which can be experienced due to earthquake activities may vary from 10^{-11} rad/s for teleseismic events (Igel et al. 2006) to up to tenths of radians per second for very strong near-field events (Nigbor 1994; Graizer 2006c). So far only large ring lasers are able to cover the lower end of the measurement range adequately. Despite of the high performance level of the ring lasers, there are a few substantial drawbacks in using these instruments for seismic measurements. They require a good laboratory environment in purpose built facilities and recurrent adjustments and maintenance. This holds even for instruments designed for seismic research applications (Schreiber et al. 2006). The relocation of such devices is relatively difficult and time-consuming. Hence, it is desirable to supplement the very broadband measurements of ring lasers with less precise but mobile, robust, and cost-effective solutions based on FOG technology.

Such rotation sensing units cover the upper bound of the seismic signals range providing the measurements around all three axis simultaneously, if three devices are put together orthogonally to cover all degrees of freedom of rotation.

Modern FOG realizations can have an upper rotation detection limit of several radians per second in closed loop operations, and their sensitivity to rotation reaches down by about 5 orders of magnitude. Depending on the application in mind, FOGs can be configured for different upper limits but cannot go below 5.5×10^{-8} rad/s because of the shot noise limit. Their theoretical bandwidth of use can be as high as several hundreds of kilohertz (Lefevre 1993); however, in practice, they are usually limited to few hundreds of hertz or about 4 kHz, which again depends on the desired application. This is more than enough for all practical purposes of strong motion sensing. The most important issue in the application of FOGs is an accuracy limitation of the rotation sensor, which is analyzed in the following chapter.

4 Analysis of fiber optic gyroscope accuracy

Prior to operation, any inertial sensor must be calibrated in order to define its operation parameters and accuracy characteristics, such as scale factor, stability over time and temperature range, output signal linearity, noise level, etc. This process is standardized, and all the required test steps are summarized in the Institute of Electrical and Electronics Engineers (IEEE) standards for corresponding instrument types (IEEE-952 1998). Manufacturers usually provide the most important characteristics in the sensor specification sheet, but these quantities are familiar to navigation engineers rather than seismologists. Here we review the relevant parameters, which are important for the field application of the fiber optic gyroscope with respect to seismological needs.

A generally accepted method for the characterization of the performance of inertial sensors is the Allan variance (Allan 1966). Initially developed for the analysis of the frequency stability in precision oscillators, this method allows a quantitative determination of noise processes in any continuous signal. For practical purposes, the result of this

signal analysis is usually represented in the form of the Allan deviation (ADEV) $\sigma(\tau)$ vs. averaging time τ because the ADEV has the same units as the signal under test. In the case of a rotation sensor, a typical curve plotted in the conventional logarithmic scale is presented in Fig. 1. Different types of noise contributions contained in the signal give rise to distinct slopes of the ADEV and therefore allows individual noise processes to be identified. Furthermore, its numerical parameters can be taken from the plot directly. In this example, $Q = 0.577''$ is the quantization noise due to the digital output of the sensor, $N = 0.001^\circ/\sqrt{h}$ is the random walk of the angle, $B = 0.001^\circ/h$ is the bias instability, and $K = 0.0001^\circ/h/\sqrt{h}$ is the rate random walk. All parameters are expressed in degrees per hour as this is the accepted convention in navigation (IEEE-952 1998). We now take a closer look at those parameters which are relevant to measurements in seismology.

4.1 Angle random walk

The part of the curve with a slope of -0.5 characterizes the white noise contained in the measured rotation rates or, if integrated over time—the angle random walk. The origin of this error source in the sensor output is the spontaneous emission of photons (shot noise). The numerical parameter of the angle random walk can be obtained by fitting a straight line through the part of the signal which

corresponds to a slope of -0.5 and taking its value at $\tau = 1$. The ADEV of our instrument under test is shown in Fig. 2. The corresponding angle random walk is 4.2×10^{-6} rad/s/ $\sqrt{\text{Hz}}$ or $0.015^\circ/\sqrt{h}$ as given by manufacturer. This parameter describes the sensor accuracy limit caused by the white noise contained in the rotation rate signal. It quantifies the rate of growth of the integrated signal (angle) as a function of time, i.e., the obtained value of 4.2×10^{-6} rad/s means that corresponding angular error (standard deviation) will be 1.3×10^{-5} rad after 10 s and 2.5×10^{-4} rad after 1 h. This value is the fundamental limitation to any angular measurement application and therefore a very important parameter characterizing the ultimate sensor sensitivity. Due to the random nature of this noise process, which is an inherent property of light, this error cannot be corrected in post-processing and the resulting angular errors are impossible to model. The noise component of the output signal in a fiber optic gyro can be reduced technologically, so the appropriate sensor choice is necessary.

4.2 Bias instability

Bias instability is more commonly referred to as drift and is responsible for erroneous angular information after the integration of the gyro output signal. Contrary to a constant bias, which once established during a sensor calibration can be

Fig. 1 An example of a typical Allan deviation for a hypothetical gyroscope according to the IEEE specification format guide

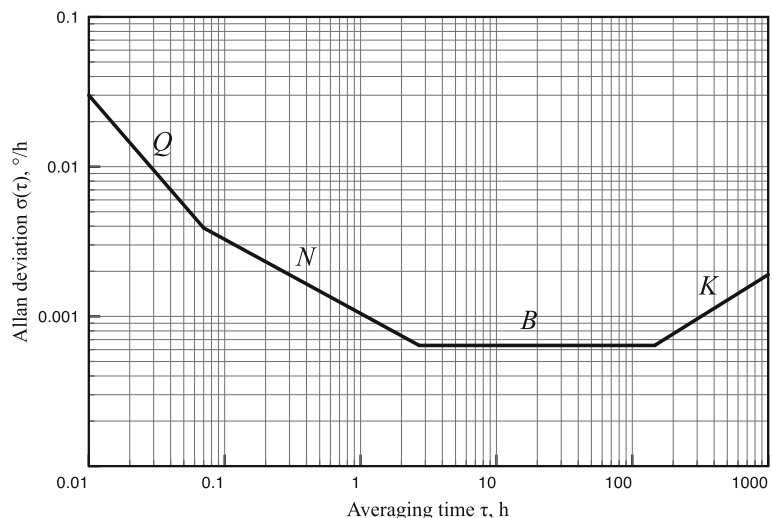
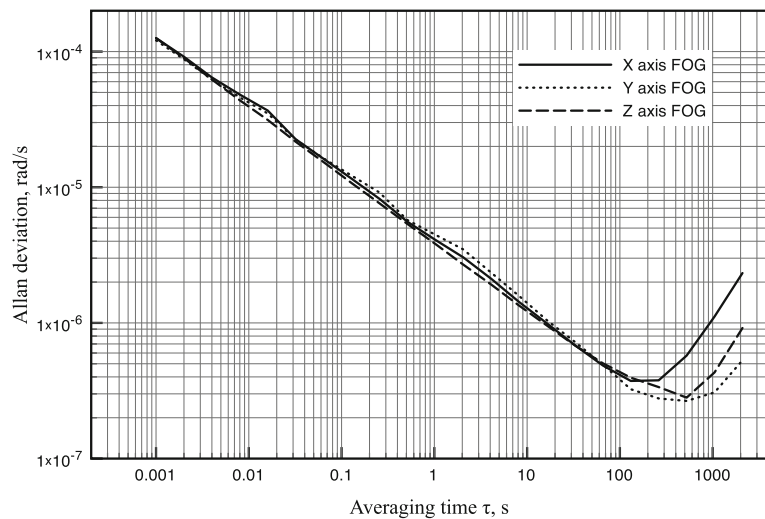


Fig. 2 ADEV for the fiber optic gyroscopes (model VG-951 by Fizoptika) under test



compensated later by subtracting its value from the data set, the bias instability accounts for the long-term variation of the sensor biases. In a typical FOG, this error is usually caused by flicker noise that originates from sensor electronics. In the ADEV, the parameter related to bias instability B can be obtained by reading the lower value of the zero-slope part of the curve $\sigma(\tau_c)$ in Fig. 1 where τ_c is the correlation time. The actual value of bias instability can then be calculated as $B = \sigma(\tau_c)/0.66428$. For the FOG under test, this value is 5.7×10^{-7} rad/s at correlation time of 200 s. It shows the best achievable stability of the individual device. Since this error reveals itself over long averaging times, it should be taken into account when measurements of long-period variations of angular position are carried out. This is especially important for monitoring long term tilt variations on site or determination of baseline corrections.

4.3 Scale factor linearity

For the interferometric fiber gyroscope, the output signal is proportional to $\sin(\Delta\varphi)$. Therefore, at large values of the input rotation rate Ω , the scale factor becomes substantially nonlinear. However, for seismic applications, where only small rotations around zero are expected, this nonlinearity does not cause significant measurement errors. More important may be the influence

of temperature variations on the FOG output signal. The accuracy parameters discussed above usually are measured under constant temperature conditions. However, the variations of these parameters with temperature may be rather large, and therefore, they should be given in the data sheet of the sensor. In the case of a FOG, where temperature gradients may affect the performance substantially, one should know the temperature operation range and fluctuations of scale factor and bias variations within that range. For the gyro under test, the operation temperature range is defined between -30°C and $+85^\circ\text{C}$ and the corresponding scale factor variations lie within 3–8%, while bias variations may reach a value of 7×10^{-7} (rad/s)/ $^\circ\text{C/h}$. It is also important to note that within the full temperature operation range, the random walk parameter may be an order of magnitude worse over the value at a fixed temperature.

4.4 Triad configuration: cross-coupling errors

Modern navigation systems are usually based on inertial measurement units—triaxial packages of accelerometers and gyroscopes. Due to the manufacturing limitations, these triaxial units possess cross-coupling errors, which arise from the misalignment of the sensitive axes of the sensors with respect to the body frame axes. These misalignments can be estimated during calibration

procedures and are expressed in terms of Euler angles Ψ_x, Ψ_y, Ψ_z . By using a traditional three-turn sequence around the z, y - and x -axes, which transforms body frame to sensors axes frame, the output signals of the gyro triad can be described as:

$$\begin{pmatrix} \omega_x^g \\ \omega_y^g \\ \omega_z^g \end{pmatrix} = \begin{bmatrix} 1 & \Psi_z & -\Psi_y \\ -\Psi_z & 1 & \Psi_x \\ \Psi_y & -\Psi_x & 1 \end{bmatrix} \begin{pmatrix} \omega_x^b \\ \omega_y^b \\ \omega_z^b \end{pmatrix} \quad (2)$$

where $\omega_i^g, i = x, y, z$ are rotation rate components sensed by each gyro and $\omega_i^b, i = x, y, z$ are components of the input rotation rate, referenced to the triad body frame. The misalignment angles Ψ_x, Ψ_y, Ψ_z are small (usually less than 10–15 arc sec); hence, the misalignment matrix has the simplified form in Eq. 2. The triad that we used for our experiments has a misalignment of 13", which leads to cross-coupling errors at the level of 62 ppm.

5 Experimental setup

The main goal of the experiment reported here is to test the suitability of tactical grade fiber optic gyros with respect to the measurements of small angular variations as they appear in applications of seismology for moderate excitation signals. Another goal was the investigation of the influence of a variable tilt on the output signal of the seismic accelerometer (EpiSensor FBA ES-T) and to develop the corresponding correction scheme. For this purpose, the calibration test bench USG-3M for reproducing of the vibrational motion was used. This apparatus allows for the production of two types of motion: a pure linear and angular motion. The latter is realized as a pendulum oscillator with an equivalent arm length of 10 m. The top platform of the test bench can move in one direction with amplitudes of linear displacement within the range of $10^{-6} \dots 10^{-2}$ m and oscillation frequencies within the range of 0.001 ... 1 Hz (angular motion) and 0.001 ... 30 Hz (linear motion). For angular motion, the uncertainty in amplitude reproduction is $0.01\phi + 3 \times 10^{-8}$ rad, where ϕ is the assigned amplitude. A small Michelson interferometer provides the information about the pure linear motion of the platform, which is trans-

ferred to the computer via a datalink. The whole installation is located inside a magnetic-isolated chamber and is placed on a independent and isolated foundation.

The three fiber optic gyroscopes were assembled into a triad with their sensitive axes orientated perpendicular with respect to each other. This provides a complete angular measurement of the platform motion. The triaxial seismic accelerometer was installed on top of the triad, its axes of sensitivity being orientated parallel to the axes of the fiber optic gyro assembly. The mutual alignment of both sensors was held within $\pm 1^\circ$, which corresponds to relative error of about 1.5×10^{-4} and can be considered as insignificant. The drawing in Fig. 3 provides a schematic view of the actual installation. Here the fiber optic gyro triad is oriented in such a way that the X -axis of the triad should detect the platform angular oscillations while Y - and Z -axis will show little or no signal. The translational signal of the accelerometer should be observable in its X -axis while the tilt-induced contribution of gravity may be very weakly visible in its Z -axis. Figure 4 shows the installation of the fiber optic gyro triad and seismic accelerometer on the moving platform of the test bench.

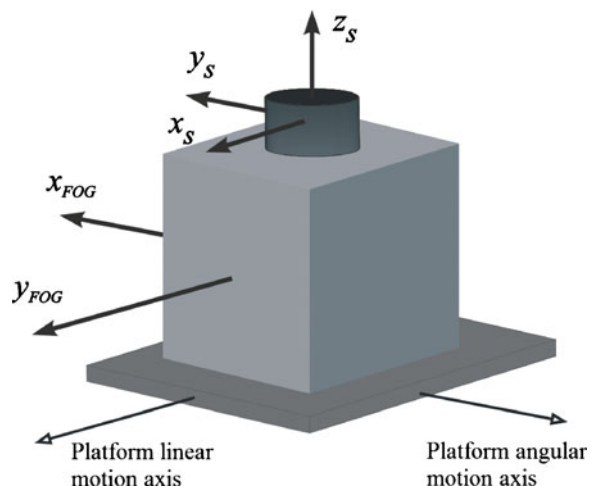


Fig. 3 Experimental setup: The FOG triad and seismic accelerometer are installed on top of the test bench platform. The X -axis of the triad is oriented along with the angular motion axis of the platform. The Y -axis of accelerometer lies in the direction of linear motion

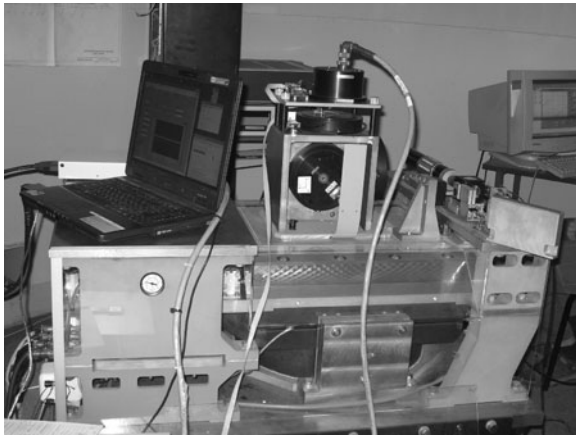


Fig. 4 Installation of the FOG triad and seismic accelerometer on the USG-3M test bench platform. The USG-3M is on the *lower part* of the photo, where the interferometer can be seen on the *right side* of the test bench, and its *left side* is occupied by the data acquisition laptop. In the *middle part* of the picture, one can see the FOG triad (grey cubical structure with *black disks* (single axis FOGs) attached to it); on *top* of this structure, the EpiSensor is mounted (*black cylinder* with thick cable). The platform motion occurs along the *horizontal axis*, parallel to the image plane

In order to start the test operation, the excursion amplitude L_0 and frequency f of the test bench platform motion was set via the control system. The motion characteristics then can be expressed as follows:

$$L_d = L_0 \sin(2\pi ft) \tag{3}$$

The corresponding angular motion therefore is:

$$\phi = L_d/R \tag{4}$$

where $R = 10$ m is the equivalent pendulum arm length. Therefore, the expression for angular rate can be written as:

$$\omega = L_0/R \cdot 2\pi f \cos(2\pi ft) \tag{5}$$

The actual acceleration along the platform axis of motion then can be written as:

$$A_\Sigma = g\phi - (2\pi f)^2 L_0 \sin(2\pi ft) \tag{6}$$

The first term in Eq. 6 shows the contribution of gravity to the accelerometer signal, while the second term describes the translational acceleration. These two vector quantities are projected onto the accelerometer axes of sensitivity, but due to

the very small magnitude of the tilt angle ($\phi_{\max} = 0.001 \ll 1$), its trigonometric function value can be substituted by the angle itself ($\sin(\phi) \approx \phi$) and $\cos(\phi) \approx 1$).

Three different types of test runs were carried out in total, namely

- Pure linear motion of the platform
- Angular motion with fixed rotation rate
- Angular motion with fixed oscillation frequency

The first run served the purpose of scale factor calibration and linearity check of the accelerometer. The test sequence contained 11 runs with frequency steps from 0.3 to 5 Hz and displacement amplitudes decreasing by $1/f^2$ to keep a constant acceleration amplitude of about 2.5×10^{-3} m/s².

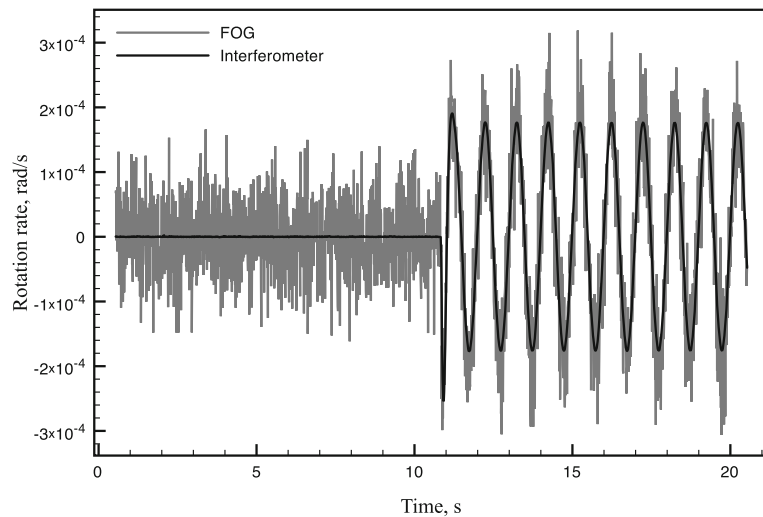
The second type of measurement was checking the response of both sensors under a constant rotation rate amplitude (approximately 1.7×10^{-3} rad/s), which has been achieved by varying both amplitude and frequency of oscillation—from 0.01 to 0.0027 m and 0.3 to 1 Hz, respectively. The third measurement sequence operated at a fixed frequency of 1 Hz, but varying rotation rate amplitudes from 1.75×10^{-4} to 5.15×10^{-3} rad/s.

The output signals of the FOG triad and seismic accelerometers were recorded along with the signal of the linear interferometer of the test bench, which provides the necessary reference for further comparisons and calibrations. The additional data processing included filtering and decimation of the FOG and the seismic accelerometer data to 100 samples/s (the acquisition rate of USG-3M interferometer datalink).

6 Experimental results

The accelerometer linearity check demonstrated an excellent agreement with the specified data of the manufacturer (though for a single axis only due to the installation limitations). The average scale factor is well within $\pm 0.5\%$ range from the factory calibrated value and its linearity varies less than ± 0.5 dB within our limited bandwidth (0.3 . . . 5 Hz). The FOG triad produced no output as expected, since translations are not generating a signal in an optical Sagnac interferometer.

Fig. 5 Rotation rates obtained by the FOG and the interferometer data for $\omega = 1.7 \times 10^{-4}$ rad/s. The first half of the measurement was taken with the system at rest

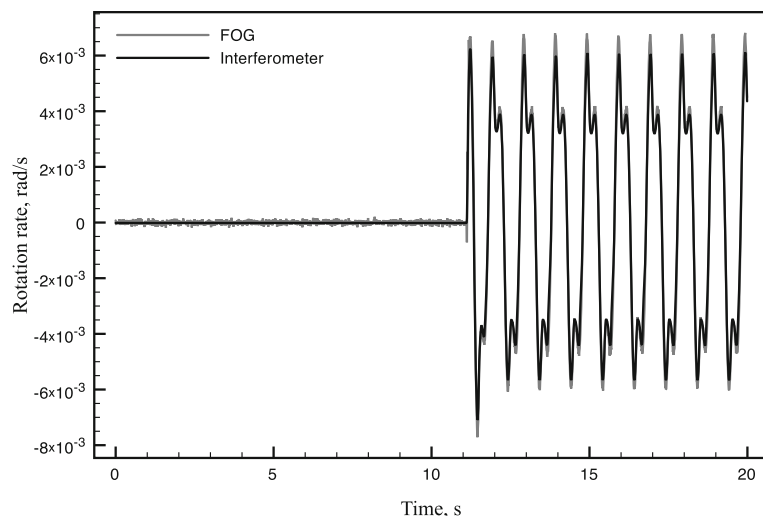


During the second test sequence, we were able to estimate the scale factor of the FOG, whose sensitivity axis was situated along the platform rotation axis. Its average value was well within the manufacturer specified value; however, the scale factor nonlinearity was found to be somewhat higher than the value specified (0.2% vs. 0.1%). This may be related to the difference in the calibration procedures. In our case, we used various rotation rates at different frequencies, while the usual calibration routine at the factory implies a number of constant rotation sequences within the whole dynamic range of the instrument. The latter method gives smoother output characteristics.

The smallest and largest variations of rotation rate as sensed by the fiber optic gyro and calculated from interferometer data in accordance to Eq. 5 and the results are shown in Figs. 5 and 6, respectively.

As one can see in Fig. 6, the peaks of rotation rate signal, albeit expected to be purely sinusoidal, are substantially distorted. This is due to the test bench being driven in off-design mode. While the platform still can operate at 1 Hz, the certified frequency operation range for angular motion is 0.001...0.5 Hz. At higher frequencies, the control system of lateral air-suspended guides (which provide the linearity of the platform motion) is not re-

Fig. 6 Rotation rates obtained by the FOG and the interferometer data for $\omega = 5.15 \times 10^{-3}$ rad/s. The first half of the measurement was taken with the system at rest



acting fast enough. This disturbs the motion of the platform at its zero crossing point. The purpose of setting the angular oscillation frequency beyond its maximal value was to obtain the highest possible rotation rate.

Both test runs 2 and 3 demonstrated good agreement between reference rotation rate variations obtained from the interferometer and FOG. In the region of lower rotational amplitudes $\omega \leq 1 \times 10^{-5}$ rad/s, the FOG signal is dominated by its noise. This is basically where the FOG meets its threshold, corresponding to the angle random walk magnitude read from Allan curve at $\tau = 0.01$ (100 Hz—data acquisition sampling rate).

During complex ground motions that also contain variable tilt contributions, the seismometer will also become sensitive to gravity. In order to estimate this component, one needs information about the tilt angle, which can be obtained from a dedicated angular rate sensor, which is not sensitive to linear motion, i.e., a fiber optic gyroscope.

Although a large volume of data were collected during the experiments, we present the results for a single selected run as an example only. This is still representative in terms of FOG performance. The linear motion amplitude was set to 4.88 mm and the frequency to 0.6 Hz, which translates into the angular rate amplitude of $\omega = 1.83 \times 10^{-3}$ rad/s.

First of all, the reference variations of the platform angular position have been calculated ac-

ording to Eq. 4. Then by taking the integral of FOG output signal, we obtained the variations of the same angle with time. An example of the angular variations according to the reference and fiber optic gyro data is shown in Fig. 7. As one can see, the angular position variation trace obtained from the FOG shows a drift, which is shown in greater detail as the difference between reference angle and FOG-derived angle (Fig. 8). This drift is the manifestation of the random walk, explained in Section 4.1, and shows the limit of sensitivity of the rotation sensor under test. The corresponding measurement error amounts to about 2.57×10^{-5} rad (standard deviation).

We now demonstrate how this may affect the seismometer tilt correction. The tilt introduces itself as an additional contribution of gravitational attraction to the output signal of the seismic accelerometer. The interferometer of the test bench delivers the pure linear displacement of the platform, hence acts as the reference for the expected acceleration and is obtained by double differentiation of this displacement. This is the signal that should be measured by the accelerometer; however, the additional tilt from the platform provides an additional term proportional to gravity. By accounting for the location of the seismic accelerometer 30 cm above the platform surface, we can calculate the reference acceleration and compare it directly with the output of the EpiSensor. Both signal traces are shown in Fig. 9.

Fig. 7 Angular variations according to FOG and interferometer data

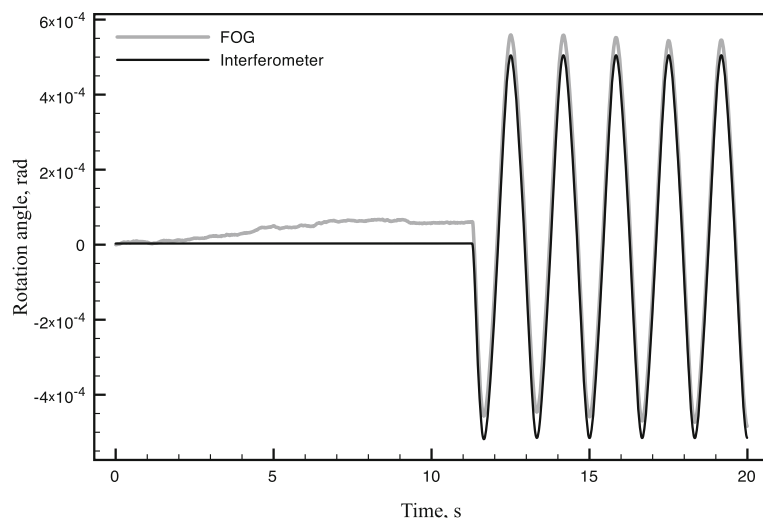
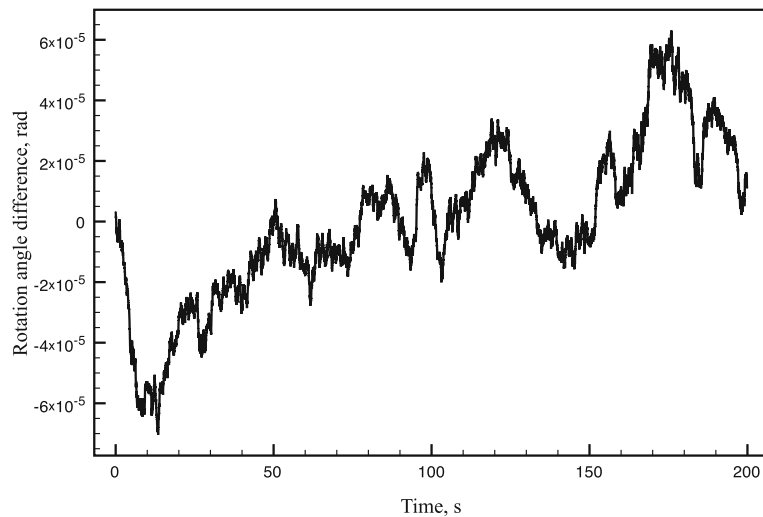


Fig. 8 Difference in angle between FOG and reference interferometer for the whole test run



The two traces have a slight mismatch on top of the oscillation amplitudes (extreme point of pendulum like motion). The residual signal, obtained by taking the difference between the reference acceleration and acceleration recorded by the EpiSensor, should be equal to the gravity contribution $g\phi$ (according to Eq. 6). This residual signal as well as the gravity-induced signal, obtained by using the FOG-derived angular motion, is shown in Fig. 10. Both traces show rather good agreement, which means that most of the tilt-induced acceleration can be compensated by using angular motion information obtained from the FOG. For this particular test, the relative error

of the gravity-induced term estimation is 5.3%. However, this error may become unacceptably large, once lower rotational rate amplitudes are experienced. Table 1 lists the dependence of the angular motion error and consequently the gravity contribution estimation error from the actual rotation rate.

The second column of Table 1 shows good agreement with the predicted angular error due to the FOG random walk (approximately 5.6×10^{-5} rad/s for 180 s). It is also clear that for rotation rates below 1×10^{-3} rad/s, the error in the estimation of the tilt-induced gravity contribution to the full acceleration measurement becomes

Fig. 9 Acceleration as a function of time measured both with the EpiSensor accelerometer and the reference interferometer of the measurement platform

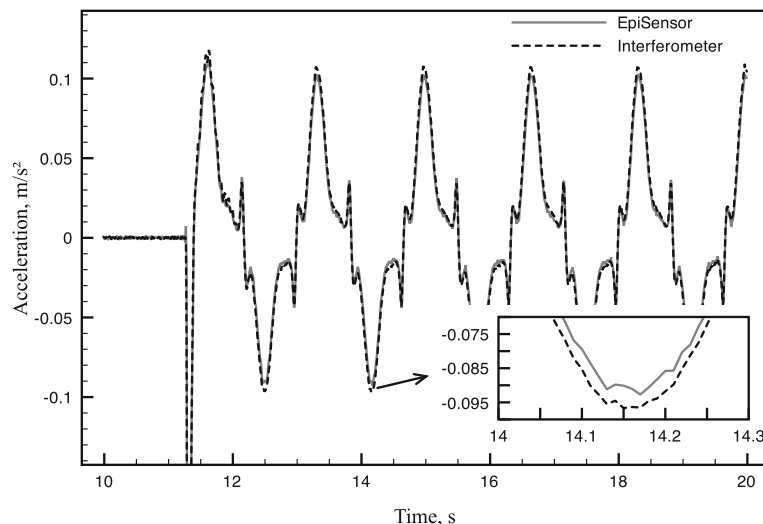


Fig. 10 Residual acceleration and gravity contribution $g\phi$, calculated by using angular variations obtained from FOG

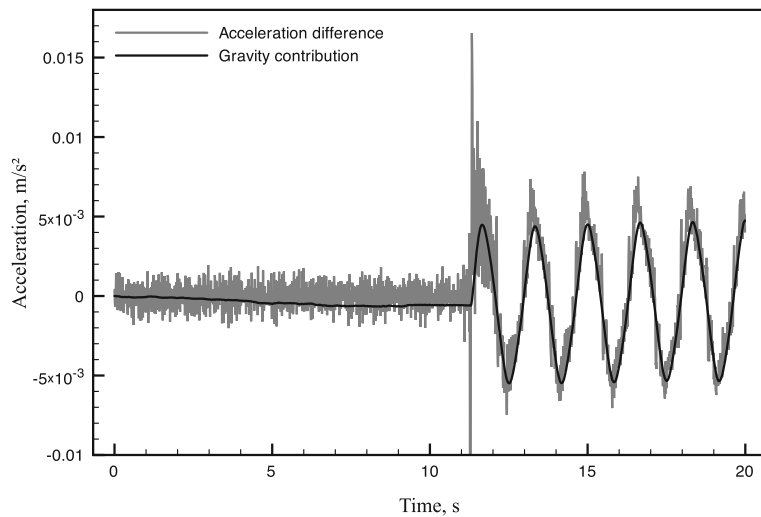


Table 1 Results from the third test run with variable rotation rate ω : angle derivation error (1σ), corresponding error in gravity contribution estimation, absolute (1σ), and relative

ω , rad/s	$\sigma\phi$, rad	$g\sigma\phi$, m/s ²	Relative error, %
1.75×10^{-4}	1.64×10^{-5}	1.61×10^{-4}	59
3.14×10^{-4}	2.29×10^{-5}	2.25×10^{-4}	46
6.26×10^{-4}	3.70×10^{-5}	3.70×10^{-4}	38
1.55×10^{-3}	1.94×10^{-5}	1.90×10^{-4}	7.8
2.75×10^{-3}	2.85×10^{-5}	2.80×10^{-4}	6.5
5.15×10^{-3}	5.12×10^{-5}	5.00×10^{-4}	6.2

unacceptably large. The worst-case scenario in our experiments is illustrated in Fig. 11, where the error of angular motion derived from the FOG is comparable in size with the reference signal amplitude.

7 Real-world application

A similar single axis FOG manufactured by LITEF GmbH, Germany (type μ FORS1) has been mounted to the second floor of the eight storey Rutherford building on the campus of the University of Canterbury, Christchurch, New

Fig. 11 Angular variations according to FOG and interferometer data for $\omega = 1.75 \times 10^{-4}$ rad/s

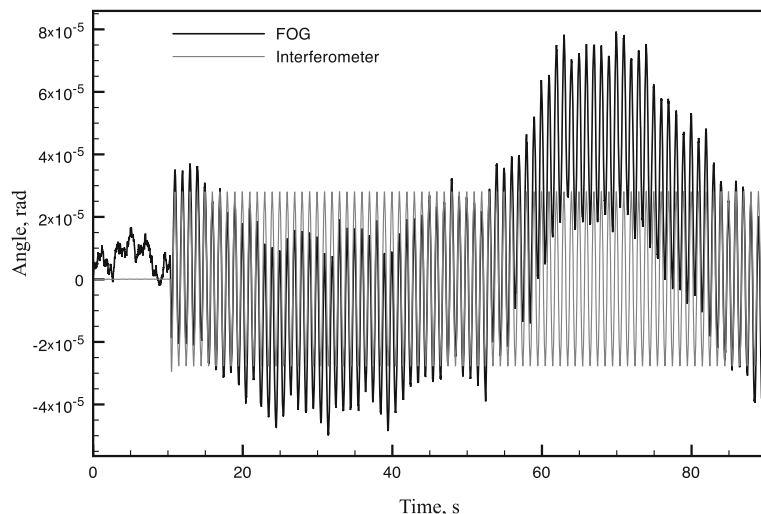
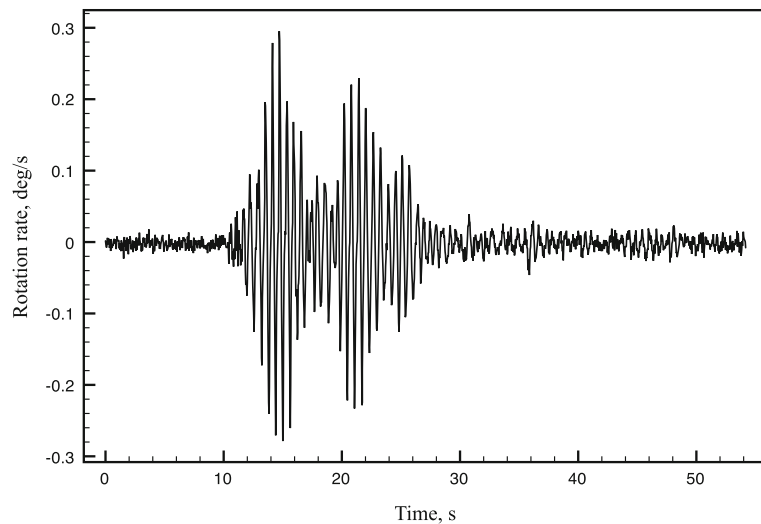


Fig. 12 Observed rotation rate from the mag. 5.3 earthquake event near Christchurch. The FOG was mounted on a shear wall in the second floor of the Rutherford building on the Campus of the University of Canterbury



Zealand. During the recent earthquake swarms, following the initial mag. 7.1 Darfield earthquake from September 4, 2010, some smaller earthquakes were recorded with this device, which was orientated such that it measures rotations around the short horizontal axis of the building. A mag. 5.3 event several kilometers away from the university campus was recorded on April 16, 2011 is presented here. Figure 12 shows the obtained rotation rate. Once the obtained rotation rates were integrated and the constant contribution to the angle caused by Earth rotation was removed, Fig. 13 was obtained. The uneven baseline of the measurement signal is caused by the random walk

contribution of the FOG in the presence of weak rocking excitations and is consistent with the sensor specification. From the excursions shown in Fig. 12 as well as from the corresponding spectrum displayed in Fig. 13, one can see that the building acts as a bandpass filter. Only frequencies around the first resonant mode of the building (rocking) amounting to ≈ 2.7 Hz have been picked up by the structure (see Fig. 14). This resonance frequency of 2.7 Hz has been independently established by ring laser measurements, evaluating building rocking from the sensor noise of a vertically mounted ring laser. The maximum amplitude of the excursion at the top floor was

Fig. 13 Observed tilt of the Rutherford building. One can see the random walk effect of the gyro on the baseline of the sensor recording

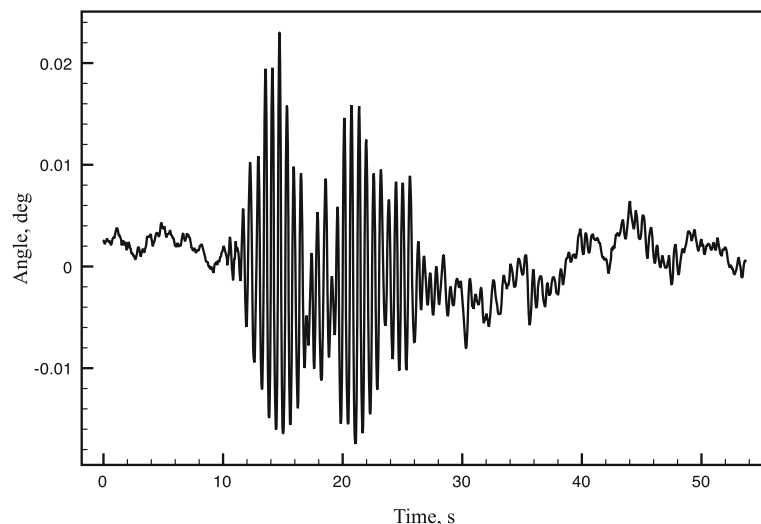
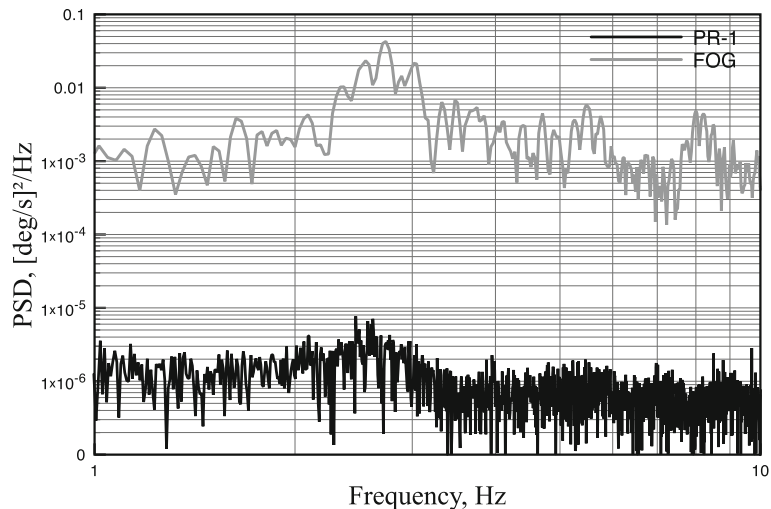


Fig. 14 Power spectral density of rotational signal recorded by FOG during the mag. 5.3 earthquake near Christchurch (*gray curve*). The spectral resolution is limited because of the short duration of the event. The *black curve* represents the background noise in the absence of an earthquake at the same location as recorded by the ring laser gyroscope PR-1



approximately 1.2 cm during this event. One can see that the signal-to-noise ratio of the FOG is entirely adequate for this application. There is sufficient dynamic range left to cope with strong motion excitations. It is also interesting to note (see Fig. 12) how the building continues to ring after the earthquake has already stopped.

8 Discussion and conclusions

In this paper, we presented the results of a fiber optic gyro triad tested with respect to small angular variation measurements. The main goal here was to estimate the abilities of a relatively inexpensive sensor to deliver reliable rotation rate data, which could be used for seismic data measurements and tilt corrections of seismometer data. The tactical grade fiber optic sensor (drift rate not better than $1^\circ/\text{h}$) is able to deliver rotation rate variations down to 1×10^{-5} rad/s and resolve small angular variations down to 10^{-6} rad. However, the quality of this particular FOG output signal is far from what is required for accurate tilt correction of seismometer data. The major problem appears to be the large magnitude of the random walk, which produces slowly varying fluctuations in resulting angular motion traces. Hence, a better sensor design is required in order to avoid this difficulty. The simulated noise analysis shows that with a random walk being 10 times lower than that of the tested gyroscope, the

angular error would be as low as 5.6×10^{-6} rad, and the gravity-induced term estimation error could be reduced to a few percent or even less over the entire range of rotation rate amplitudes in these tests. Therefore, the exhaustive estimation of angular information accuracy desired for a particular application is required before the sensor assemblage and deployment. The rule of thumb for a rotation rate sensor selection would be a residual drift value at the level of $0.1^\circ/\text{h}$ (5×10^{-7} rad/s) or below. Lower-grade sensors will eventually produce substantial angular errors, creating unreliable correction signals.

During our experiments, we reproduced a rather simple scenario of tilted motion and its consequences for the seismic measurements. Under strong excitations, the ground motion will be much more complex, having all 6 degrees of freedom. In this case, the more thorough tilt correction algorithm should be developed and implemented. The basis for its development is well established in the area of inertial navigation, and some successful implementations for seismology have been already reported (Lin et al. 2010).

A careful calibration of fiber optic gyro is required in order to guarantee reliable output signals within the expected operation range. This includes the determination of scale factor and its nonlinearity, constant bias corrections, misalignment angles in the sensor triad configuration and temperature-induced drifts. These tasks should be made on certified calibration equipment, sim-

ilar to that used in production of inertial measurement units. The lack of knowledge regarding sensor parameters and behavior may yield erroneous interpretation of results obtained during measurements.

Another challenge may be a synchronization of gyro output data with a GPS-locked time-server, which is necessary due to the strict timing requirements for seismological instrumentation. Most of the precise fiber optic gyroscopes utilize the asynchronous serial digital interface for data acquisition. Hence, precise time stamping of a recorded signal becomes a difficulty in a real-world application since there must be no unambiguity in data detection times. This problem may be solved by time stamping the acquired data on the host computer side, providing the data stream has no undue interruptions and the transfer delay is either negligible or known.

Despite of all the difficulties named above, the fiber optic gyroscope remains a good candidate for strong seismic motion detection as could be demonstrated with measurements during earthquakes in the Rutherford building in Christchurch. Theoretically, the ultimate advantages of fiber optic rotation sensors are high resolution and bandwidth, output linearity, and complete insensitivity to translational motion. The practical aspects of this kind of sensor implementation in seismology require further research, but existing preliminary test results are very promising. The experience accumulated in the inertial navigation community may be extremely helpful in resolving some more specific difficulties and establishing a proper configuration of rotation measurement systems for strong motion seismology.

Acknowledgements This research was supported in part by grant from the Federal Targeted Programme “Scientific and scientific-pedagogical personnel of the innovative Russia in 2009–2013” of the Ministry of Education and Science of the Russian Federation. We acknowledge the support of Matthew Pannell, who implemented the FOG monitoring system in the Rutherford building.

References

- Allan DW (1966) Statistics of atomic frequency standards. *Proc IEEE* 54:221–230
- Aronowitz F (1999) Fundamentals of the ring laser gyro. In: *Optical gyros and their application*. RTO AGAR-Dograph 339:3-1–3-45
- Boore DM (2001) Effect of baseline corrections on displacements and response spectra for several recordings of the 1999 Chi-Chi, Taiwan, earthquake. *Bull Seismol Soc Am* 91(5):1199–1211
- Cowsik R, Madziwa-Nussinov T, Wagoner K, Wiens D, Wyssession M (2009) Performance characteristics of a rotational seismometer for near-field and engineering applications. *Bull Seism Soc Am—Special Issue on Rotational Seismology* 99(2B):1181–1189
- Graizer V (2006) Equation of pendulum motion including rotations and its implications to the strong-ground motion. In: Teisseyre R, Majewski E, Takeo M (eds) *Earthquake source asymmetry, structural media and rotation effects*. Springer, Berlin, pp 471–485
- Graizer V (2006b) Theoretical basis for rotational effects in strong motion and some results. In: *Rotational workshop*, 16.02.2006. Menlo Park/Pasadena, CA
- Grazer V (2006) Tilts in strong ground motion. *Bull Seismol Soc Am* 96(6):2090–2102
- Graizer V (2010) Strong motion recordings and residual displacements: what are we actually recording in strong motion seismology? *Seismol Res Lett* 81(4):635–639
- IEEE (1998) IEEE standard specification format guide and test procedure for single-axis interferometric fiber optic gyros. Institute of Electrical and Electronics Engineers, New York
- Igel H, Schreiber U, Flaws A, Schuberth B, Velikoseltsev A, Cochard A (2005) Rotational motions induced by the M8.1 Tokachi-Oki earthquake, September 25, 2003. *GRL* 32(8):L08,309.1–L08,309.5
- Igel H, Cochard A, Wassermann J, Flaws A, Schreiber U, Velikoseltsev A, Dinh NP (2006) Broad-band observations of earthquake-induced rotational ground motions. *Geophys J Int* 168(4):182–196
- Lawrence A (1998) *Modern inertial technology: navigation, guidance, and control*. Mechanical Engineering series, 2nd edn. Springer, New York
- Lefevre H (1993) *The fiber-optic gyroscope*. Artec House, Boston
- Lin C-J, Huang H-P, Liu C-C, Chiu H-C (2010) Application of rotational sensors to correcting rotation-induced effects on accelerometers. *Bull Seismol Soc Am* 100(2):585–597
- Nigbor RL (1994) Six-degree-of-freedom ground-motion measurement. *Bull Seismol Soc Am* 84(5):1665–1669
- Nigbor RL, Evans JR, Hutt CR (2009) Laboratory and field testing of commercial rotational seismometers. *Bull Seism Soc Am—Special Issue on Rotational Seismology* 99(2B):1215–1227
- Pancha A, Webb TH, Stedman GE, McLeod DP, Schreiber U (2000) Ring laser detection of rotations from teleseismic waves. *GRL* 27:3553–3556 (2000)
- Pillet R, Virieux J (2007) The effects of seismic rotations on inertial sensors. *Geophys J Int* 171(3):1314–1323
- Sanders G, Szafraniec B (1999) Progress in fiber-optic gyroscope applications ii with emphasis on the theory

- of depolarized gyros. In: Loukianov DP, Rodloff R, Sorg H, Stieler B (eds) *Optical gyros and their application*, vol. 339. RTO AGARD, Neuilly sur Seine, pp 11.1–11.42
- Schreiber KU, Stedman GE, Igel H, Flaws A (2006) Ring laser gyroscopes as rotation sensors for seismic wave studies. In: Teisseyre R, Majewski E, Takeo M (eds) *Earthquake source asymmetry, structural media and rotation effects*. Springer, Berlin, pp 377–390
- Schreiber KU, Carr AJ, Franco-Anaya R, Velikoseltsev A (2009) The application of fiber optic gyroscopes for the measurement of rotations in structural engineering. *Bull Seism Soc Am—Special Issue on Rotational Seismology* 99(2B):1207–1214
- Suryanto W, Igel H, Wassermann J, Cochard A, Schuberth B, Vollmer D, Scherbaum F, Schreiber U, Velikoseltsev A (2006) First comparison of array-derived rotational ground motions with direct ring laser measurements. *BSSA* 96(6):2059–2071
- Takamori A, Araya A, Otake Y, Ishidoshiro K, Ando M (2009) Research and development status of a new rotational seismometer based on the flux pinning effect of a superconductor. *Bull Seism Soc Am—Special Issue on Rotational Seismology* 99(2B):1174–1180